

## Protein crystal growth results for shuttle flights STS-26 and STS-29

Lawrence J. DeLucas <sup>a</sup>, Craig D. Smith <sup>a</sup>, Wilson Smith <sup>a</sup>, Senadhi Vijay-Kumar <sup>a</sup>, Shobha E. Senadhi <sup>a</sup>, Steven E. Ealick <sup>a</sup>, Daniel C. Carter <sup>b</sup>, Robert S. Snyder <sup>b</sup>, Patricia C. Weber <sup>c</sup>, F. Raymond Salemme <sup>c</sup>, D.H. Ohlendorf <sup>c</sup>, H.M. Einspahr <sup>d</sup>, L.L. Clancy <sup>d</sup>, Manuel A. Navia <sup>e</sup>, Brian M. McKeever <sup>e</sup>, T.L. Nagabhushan <sup>f</sup>, George Nelson <sup>g</sup>, A. McPherson <sup>h</sup>, S. Koszelak <sup>h</sup>, G. Taylor <sup>i</sup>, D. Stammers <sup>j</sup>, K. Powell <sup>j</sup>, G. Darby <sup>j</sup> and Charles E. Bugg <sup>a</sup>

<sup>a</sup> Center for Macromolecular Crystallography, P O Box 79-THT, UAB Station, Birmingham, Alabama 35294, USA

<sup>b</sup> George C Marshall Space Flight Center, Huntsville, Alabama 35812, USA

<sup>c</sup> Central Research and Development Department, E I du Pont de Nemours & Co., Wilmington, Delaware 19880, USA

<sup>d</sup> The Upjohn Company, Kalamazoo, Michigan 49001, USA

<sup>e</sup> Merck Sharp & Dohme Research Laboratories, Rahway, New Jersey 07065, USA

<sup>f</sup> Schering-Plough Corporation, Bloomfield, New Jersey 07003, USA

<sup>g</sup> Astronomy Department, University of Washington, Seattle, Washington 98195, USA

<sup>h</sup> University of California at Riverside, Riverside, California 92521, USA

<sup>i</sup> Laboratory of Molecular Biophysics, University of Oxford, Oxford OX1 3QU, UK

<sup>j</sup> Wellcome Research Laboratories, Beckenham BR3 3BS, UK

Recent advances in protein crystallography have significantly shortened the time and labor required to determine the three-dimensional structures of macromolecules once good crystals are available. Crystal growth has become a major bottleneck in further development of protein crystallography. Proteins and other biological macromolecules are notoriously difficult to crystallize. Even when usable crystals are obtained, the crystals of essentially all proteins and other biological macromolecules are poorly ordered, and diffract to resolutions considerably lower than that available for most crystals of simple organic and inorganic compounds. One promising area of research which is receiving widespread attention is protein crystal growth in the microgravity environment of space. A series of protein crystal growth experiments were performed on US shuttle flight STS-26 in September 1988 and STS-29 in March 1989. These proteins had been studied extensively in crystal growth experiments on earth prior to the microgravity experiments. For those proteins which produced crystals of adequate size, three-dimensional intensity data sets with electronic area detector systems were collected. Comparisons of the microgravity-grown crystals with the best earth-grown crystals obtained in numerous experiments demonstrate that the microgravity-grown crystals of these proteins are larger, display more uniform morphologies, and yield diffraction data to significantly higher resolutions. Analyses of the three-dimensional data sets by relative-Wilson plots indicate that the space-grown crystals are more highly ordered at the molecular level than their earth-grown counterparts.

### 1. Introduction

A number of exciting protein crystallography projects are often terminated because of the inability to obtain crystals of suitable quality for high-resolution diffraction analyses. One promising new development in protein crystal growth involves studies of crystal growth processes in the

microgravity environment obtainable in space [1,2]. The major motivation behind these space experiments is to eliminate the density-driven convective flow that accompanies crystal growth in gravitational fields [3,4]. In addition, sedimentation of growing crystals, which can interfere with the formation of single crystals, is eliminated in the absence of gravity.

The first microgravity protein crystal growth experiments were performed on Spacelab I by Litke and John [5]. These experiments indicated that the space-grown crystals, which were obtained using a liquid-liquid diffusion system, were larger than crystals obtained by the same experimental system on earth. Experiments on four space shuttle missions in 1985 and 1986 were used to develop an apparatus for protein crystal growth by vapor diffusion techniques [5]. This equipment was used in protein crystal growth experiments on US space shuttle flights STS-26 and STS-29. This paper presents the results obtained from these two flight experiments.

## 2. Hardware development

The space shuttle experiments involved crystal growth by a vapor diffusion technique, which is closely related to the widely used hanging drop method of protein crystal growth on earth [7]. This method was chosen for several reasons:

- (1) Most protein crystallography laboratories have extensive experience with this method and a large percentage of the protein crystals described in recent publications have been obtained using this technique.
- (2) This technique is particularly amenable to crystallization experiments involving small quantities of protein.
- (3) In a microgravity environment, relatively large stable droplets of protein solution can be formed with minimal surface contacts, thereby decreasing possible nucleation sites and eliminating wall effects that generally accompany crystallization experiments on earth.

The hardware was developed by using a simple piece of equipment that was easily modified and improved through a series of four shuttle missions in 1985 and 1986. Crystals are grown in 40  $\mu$ l droplets that are extruded from syringes and subsequently permitted to equilibrate with solutions of precipitating agents contained within closed chambers.

Fig. 1 shows the principle behind the design of the apparatus developed for protein crystal growth by vapor diffusion techniques. Each experiment

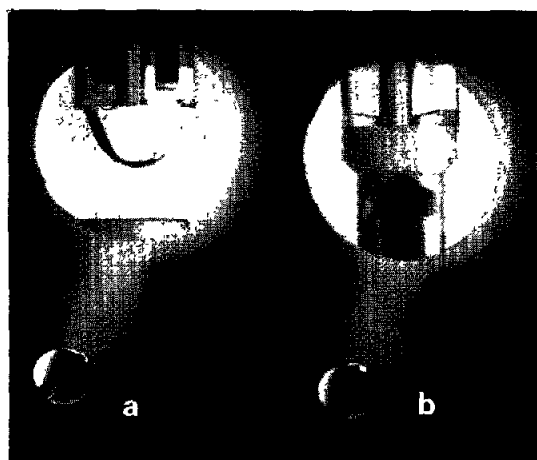


Fig. 1 Crystal growth chamber (a) unstoppered syringe with protein and precipitant solutions extruded into droplet on syringe tip, (b) stoppered syringe (configuration during launch and landing)

takes place within a sealed chamber that has a volume of  $\approx 5.3 \text{ cm}^3$  with clear plastic windows for visual and photographic monitoring of crystal growth. The back chamber windows are covered with a polarizer to enhance photography of the crystal growing within the droplets. Prior to activation of the experiment the protein solutions are contained within double barrel syringes which are stoppered during launch and landing (fig. 1b). The two barrels of the syringes are filled with protein and precipitant solution respectively. Growth is activated by withdrawing the stopper and extruding the protein and precipitant solutions simultaneously onto the syringe tip (fig. 1a). The combined protein-precipitant droplet equilibrates with a wicking material saturated with an equilibration solution. After the crystallization experiment is complete, the protein solution containing the crystals is withdrawn back into the syringe and the stopper is reinserted on the tip. One entire vapor diffusion tray with dimensions of  $35.8 \times 1.66 \times 8.6 \text{ cm}$  contains twenty crystal growth chambers (fig. 2). Three vapor diffusion trays are contained in a refrigeration incubator module (RIM) which occupies one middeck locker on the shuttle. The RIM is capable of maintaining any set temperature between  $2 \text{ and } 35 \pm 0.8^\circ \text{C}$  (fig. 3).

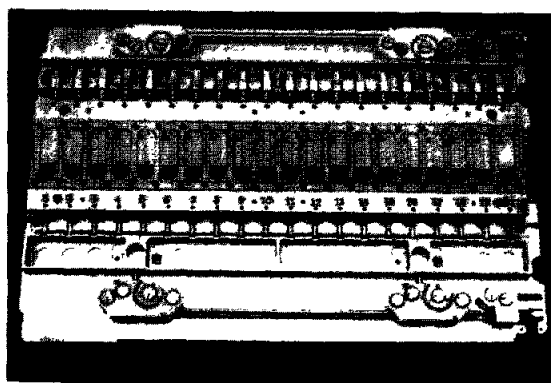


Fig 2 Vapor diffusion tray

All solutions were loaded into the shuttle equipment approximately 24 h prior to launch. Once in orbit, crystal growth was activated by extruding the solutions onto the tip of the syringe, where mixing of the protein solution and precipitating agent was achieved by repeatedly withdrawing and extruding the solutions. The suspended droplet was then allowed to equilibrate with the surrounding solution of precipitating agent. The protein droplets are photographed after activation and at 24 h intervals during the shuttle flight. At

the end of the mission, the solutions and suspended crystals are withdrawn into the syringes which are stoppered for return to earth. The experimental apparatus is contained within the RIM maintained at a temperature of  $22.8 \pm 0.7^\circ\text{C}$  from the time that the samples are loaded until the analyses of the crystals could be performed. Slightly higher temperatures occurred for short periods of time during the photographic sessions.

Immediately after the shuttle landed, the hardware was transported in the RIM to Birmingham where the analyses were initiated. The space-grown crystals were extruded into depression plates, sealed with glass coverslips and photographed using a binocular microscope. Selected crystals were sealed in glass capillaries for X-ray diffraction analysis.

Ground control experiments were performed in equipment identical to that used for the shuttle experiments. These control experiments began seven days after the shuttle landed, using the same protein solutions and identical loading, activation and deactivation times as those that were followed for the shuttle experiments. In addition, extensive control experiments were performed in prototypes

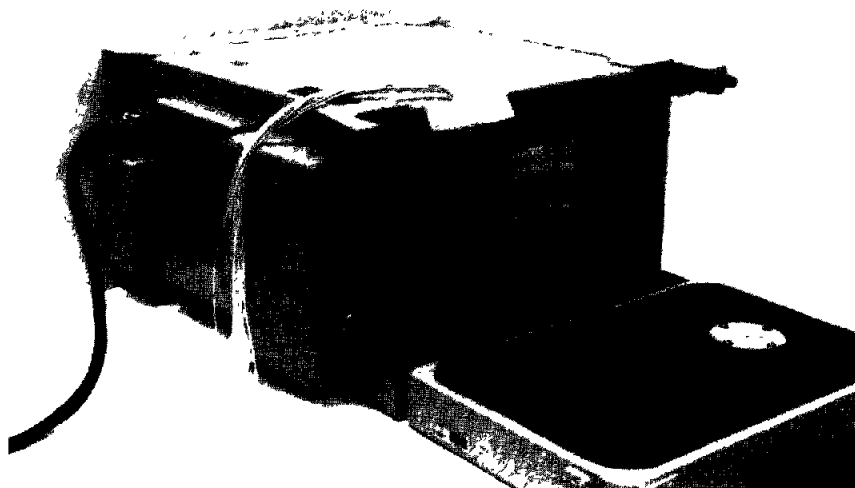


Fig 3 Refrigerator incubator module containing three vapor diffusions trays. To activate and deactivate the experiments, a ganging mechanism attached to each tray is manually operated by the astronaut. Fluctuations in temperature are recorded with a data logger via three sensors which are located under each vapor diffusion tray.

of the space shuttle hardware before and after the shuttle experiments were completed.

### 3. STS-26 analysis

X-ray diffraction photographs were obtained from a number of crystals grown in the space and ground control experiments. These photographs were obtained with crystals in stationary orientations, using specially constructed cylindrical cassettes mounted on rotating anode X-ray generators. More detailed X-ray diffraction studies were performed with Nicolet area detector systems [8], using rotating anode X-ray generators with copper targets, at the University of Alabama at Birmingham, DuPont and Merck. Three-dimensional X-ray diffraction data sets were collected from space-grown crystals of all three compounds.

The X-ray diffraction photographs obtained from crystals grown in the space and control experiments were used for qualitative evaluation of diffraction resolutions. The results from these analyses are consistent with the more detailed studies performed using three-dimensional data sets measured with the area detector systems. Since evaluation of diffraction resolutions from photographs is highly subjective, and is often dependent upon crystal orientations, we have depended primarily upon three-dimensional intensity data sets for comparison of space and earth-grown crystals. The techniques and crystal growth conditions used for the space experiments closely parallel the vapor diffusion experiments that have been used in numerous studies on earth with these three proteins. Consequently, three-dimensional X-ray diffraction data sets obtained from the space-grown crystals were compared with the best data sets that had been obtained from earth-grown crystals of these proteins using area detector systems and experimental protocols similar to those followed for obtaining data from the space-grown crystals.

Intensity data sets from crystals of these three proteins were analyzed in a variety of different ways. There are no uniformly accepted criteria for assessing the quality of protein crystals, but the general criteria of interest from a practical standpoint are assessment of the largest Bragg angles at

which usable data can be measured, and evaluation of the percentage of data above background levels throughout the data collection range. Consequently, plots were made of average  $I/\sigma(I)$  ( $I$  = intensity) values versus diffraction resolution, and percentages of data above various cut-off levels as functions of resolution. In addition, data sets from space and earth-grown crystals were compared by using Wilson plots [9]. Wilson plots can be used to estimate the overall  $B$  values for the crystals, which are related to the root-mean-square displacements at atomic positions. These  $B$  values reflect the internal order within the crystals. Wilson plots from proteins are generally difficult to interpret. However, relative-Wilson (also known as difference-Wilson [9]) plots are useful for assessing changes in the internal order of protein crystals. These plots of  $\ln(\sum F_a^2/\sum F_b^2)$  versus  $4 \sin^2\theta/\lambda^2$  are routinely used to characterize and compensate for the disordering effects resulting from the diffusion of heavy atom derivatives into protein crystals. The slopes of these plots are directly related to the difference in overall  $B$  values for two different crystals, a and b (a corresponds to the space-grown crystals and b to the earth-grown crystals in the following relative-Wilson plots).

#### 3.1 Results- $\gamma$ -interferon ( $\gamma$ -IFN D)

The STS-26 experiments included an engineered form of  $\gamma$ -IFN D. Crystals of this protein are trigonal, space group R32, with  $a = b = 114 \text{ \AA}$  and  $c = 315 \text{ \AA}$ . They are grown from a solution of 49% ammonium sulfate, 0.05M Na acetate, pH = 5.9 [10]. A large number of crystallization experiments have been performed at the University of Alabama at Birmingham with this protein over a two-year period, and several three-dimensional data sets have been collected using electronic area detector systems. Crystallization conditions for the STS-26 experiments were identical to those routinely used for crystal growth studies on earth. Several crystals were obtained that were as large as or larger than the best that have been produced in the ground experiments. One of the crystals of  $\gamma$ -IFN D grown on STS-26 was approximately 50% larger than the largest crystal that had been

obtained previously. This crystal is depicted in fig. 4. The overall morphology is similar to the earth-grown crystals, although the one depicted in fig. 1 is somewhat thicker than those routinely obtained in laboratory studies.

Three-dimensional intensity data were collected from the crystal shown in fig. 4, and these data were compared with data sets obtained from earth-grown crystals. Fig. 5a shows the distributions of observable data ( $I/\sigma(I) \geq 5$ ) from the space-grown crystal and data sets obtained from several of the best earth-grown crystals that had been obtained previously. All of the data sets from earth-grown crystals display the same general intensity pattern as a function of resolution. On the other hand, the space-grown crystal displays a significant increase in measurable data throughout the resolution range, with a significant fraction of measurable data at resolutions where the earth-grown crystals display no significant diffraction.

The intensity data set collected from the space-grown crystal of  $\gamma$ -IFN D is clearly superior to any data obtained previously. In principle, this improvement could reflect enhanced counting statistics resulting from the larger crystal volume. However, examination of a relative-Wilson plot that compares data from the space-grown crystal



Fig. 4 Crystal of  $\gamma$ -IFN D grown on STS-26. This crystal has dimensions of  $0.7 \times 0.5 \times 0.4$  mm.

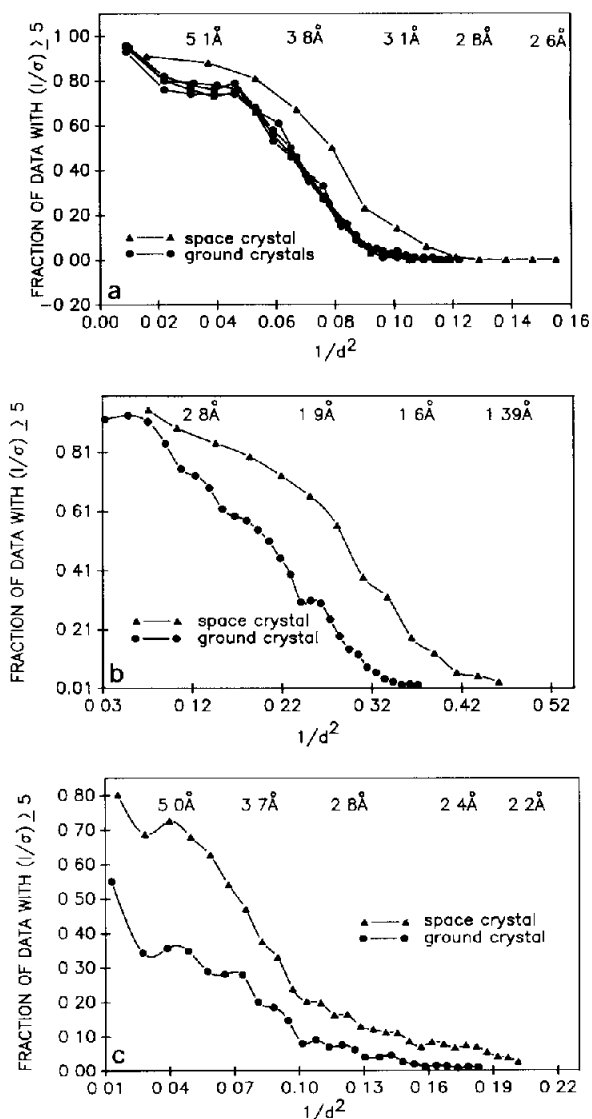


Fig. 5 Comparison of diffraction intensity data for (a) space-grown  $\gamma$ -IFN D crystal and the data obtained from four of the largest earth-grown crystals of  $\gamma$ -IFN D, (b) space-grown elastase crystal and an elastase crystal of comparable size grown on earth, (c) comparison of intensity distributions for space-grown and earth-grown crystals of isocitrate lyase.

with those from one of the better earth-grown crystals indicates that the space-grown crystal displays a lower effective  $B$  value. This relative-Wilson plot is shown in fig. 6a. If the effective  $B$  values of the two crystals were comparable, the

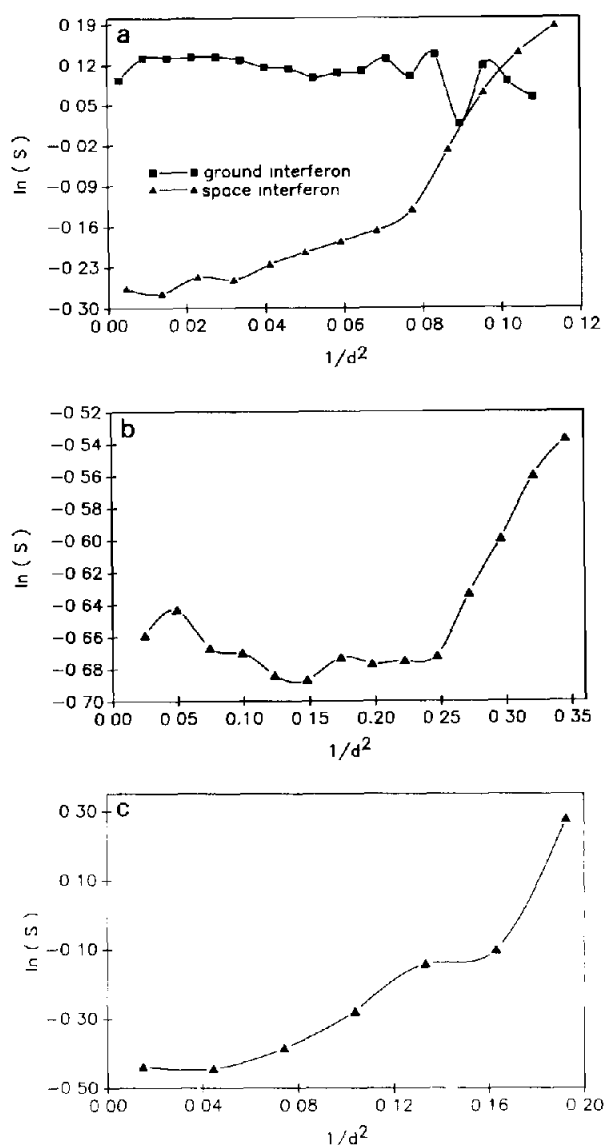


Fig. 6 Relative-Wilson plot comparing space-grown and earth-grown crystals of (a)  $\gamma$ -IFN D, (b) porcine elastase and (c) socitrate lyase. In addition, a relative-Wilson plot comparing two earth-grown crystals of  $\gamma$ -IFN D is shown in (a).

relative-Wilson plot should be flat with a slope of zero. For comparative purposes, a Wilson plot using data from two of the ground-grown  $\gamma$ -IFN D crystals is shown. The slope for this plot is essentially zero, whereas the space versus ground plot displays a positive slope throughout the resolution range, with a steeper slope at the higher resolutions, indicating that the  $B$  value for the

space-grown crystal is lower than that for the earth-grown crystal.

### 3.2 Porcine elastase

Crystals of porcine elastase are orthorhombic, space group  $P2_12_12_1$ , with  $a = 50.9 \text{ \AA}$ ,  $b = 57.2 \text{ \AA}$ , and  $c = 75.0 \text{ \AA}$ . Crystals were grown by seeding techniques from solutions of precipitant (1.5 M  $\text{NaSO}_4$ , 0.1M sodium acetate, pH = 5.0 [11]). Crystals were grown on STS-26 by adding small seed crystals to the solution of precipitating agent in one side of the double-barreled syringes. The seed crystals used were approximately  $50 \mu\text{m}$  in the maximum dimension. Fig. 7 shows a sequence of photographs obtained at 24 h intervals during STS-26 depicting growth from one of the elastase seed crystals. The seed crystal can be seen suspended within the droplet shortly after experiment activation. By the second day, the crystal has become attached to the surface of the droplet. The crystal then continues to grow into the solution during the flight. The final crystal produced in the experimental sequence depicted in fig. 7 is 2.05 mm long, which is considerably larger than any elastase crystals obtained in ground-control studies. Fig. 8 shows a typical elastase crystal obtained in microgravity. A number of well formed elastase crystals in the range 0.5–2.0 mm were obtained on STS-26. Three-dimensional intensity data were collected from a space-grown crystal that had dimensions comparable to the dimensions of earth-grown crystals studied earlier.

Fig. 5b shows a comparison between the intensity data sets from one of the space-grown crystals and an earth-grown crystal of comparable volume. The space-grown crystal of elastase produces significantly more data at all resolution ranges, with appreciable enhancement in the ultimate resolution at which measurable data can be obtained. The relative-Wilson plot comparing data from the space-grown crystal with that from the earth-grown crystal is shown in fig. 6b. This plot does not reveal a significant difference in  $B$  values for data in the lower resolution ranges, but the higher resolution data indicate that the space-grown crystal has a significantly lower overall effective  $B$  value.

### 3.3 Isocitrate lyase

Crystals of isocitrate lyase are orthorhombic, space group  $P2_12_12_1$ , with  $a = 80.7 \text{ \AA}$ ,  $b = 123.1 \text{ \AA}$  and  $c = 183.4 \text{ \AA}$ . Crystals were grown from a solution of 1.7M sodium citrate, 0.1M Tris-HCl, pH = 8.0. Crystallization experiments on earth

have invariably resulted in the growth of dendritic clusters, such as that depicted in fig. 9a.

An improved habit for isocitrate lyase was observed from the experiments on STS-26. Although some dendritic growth was found in the space samples, a number of well-formed prisms, depicted in fig. 9b, were obtained in the microgravity

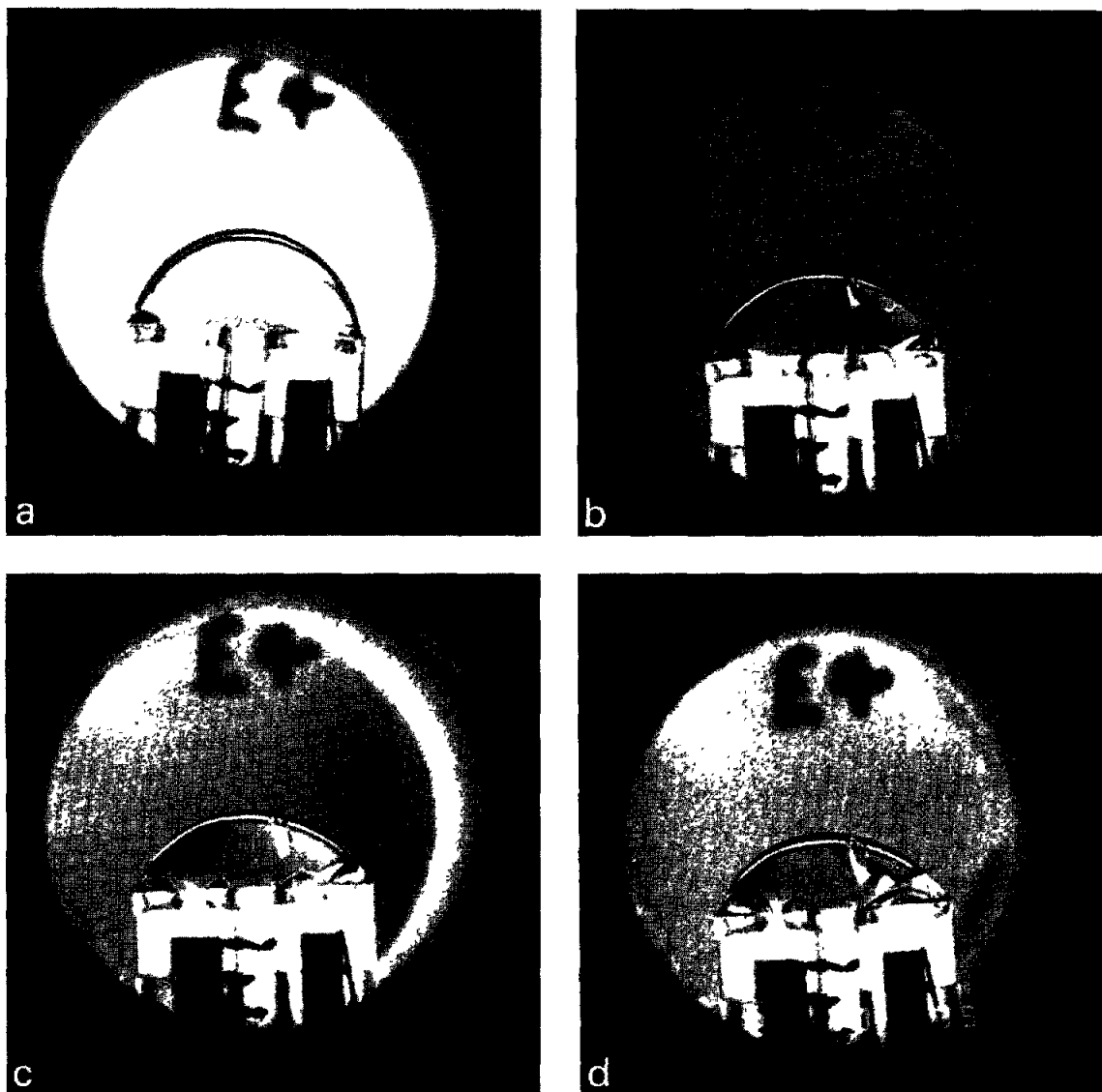


Fig 7 Crystal of porcine elastase growing in microgravity at (a) initial seeding stage, (b) end of day 1, (c) end of day 2, and (d) end of day 3 immediately before retracting the droplet and crystal into the syringe

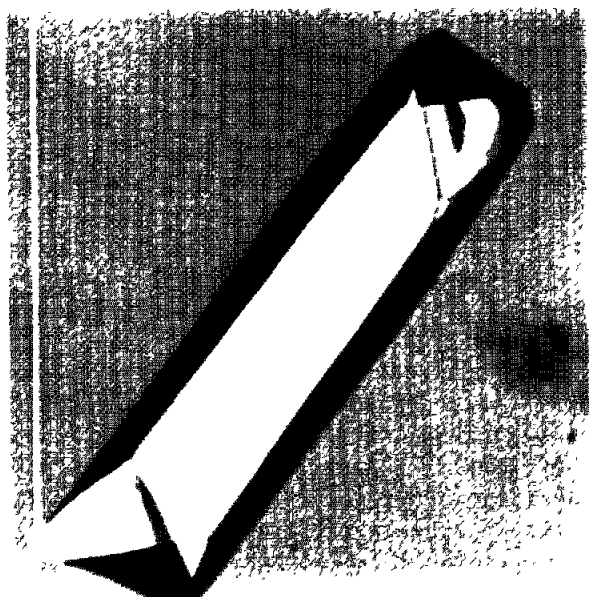


Fig. 8. Crystal of porcine elastase from the space experiment. The crystal grew from a seed and is approximately 15 mm in length. Several smaller crystals grew in the same droplet.

experiments. These prisms belong to the same space group as the earth-grown dendrites. However, they yield intensity data that are consider-

ably superior to those obtained previously. Fig. 5c compares the intensity data from a space-grown prism with one of the better data sets obtained from earth-grown crystals of isocitrate lyase. The space-grown crystal produced data of higher quality throughout the resolution range. Fig. 6c shows a relative-Wilson plot for the space-grown and earth-grown crystals of isocitrate lyase. Except at the lowest resolution range, the plot indicates that the space-grown crystal has a significantly lower effective  $B$  value than the earth-grown crystal.

Of the eight other proteins crystallized on STS-26 [12], six did not produce crystals large enough for diffraction analysis. One produced only a partial data set, the analysis of which was inconclusive when compared to earth data. The final protein (canavalin) displayed higher resolution ( $\sim 0.2$  Å) on the film data, but the 3D data could not be processed because of experimental difficulties that arose during the data collection process.

#### 4. STS-29 results

Fifteen different protein samples were flown on STS-29. Unfortunately, showers of small crystals



a



Fig. 9. (a) Typical dendritic morphology for isocitrate crystals grown on earth. The vertical and horizontal dimensions of this dendritic cluster are 0.74 mm and 0.46 mm, respectively. (b) Prisms of isocitrate lyase grown on STS-26. The crystal dimensions are approximately  $0.4 \times 0.25 \times 0.04$  mm.



were produced in every chamber flown for all fifteen of these proteins. It is not clear what caused this. In spite of this, one crystal of the protein  $\gamma$ -interferon grew large enough to collect 3D data. Although the crystal was 0.2 mm smaller in each dimension than the four earth-grown crystals used for comparison of the STS-26 data, the STS-29 space-grown crystal still produced data that were measurably better throughout the resolution range and extended further in resolution than the best ground-based crystals. The relative-Wilson plot indicated once again that the  $B$  value for the space-grown crystal is lower than that for the earth-grown crystals. In addition, three large crystals ( $\sim 0.4 \times 0.3 \times 0.5$  mm) of the protein *Lathyrus ochrus lectin I* were also obtained. Data were collected to high resolution from one of these crystals and the structure was determined by molecular replacement methods. Crystals grown on earth by similar methods are smaller and display a different habit. A detailed comparison of the space and ground data will be published elsewhere (personal communication, Juan Fontecilla, University of Marseille)

## 5. Discussion

The results from STS-26 and STS-29 indicate that when the growth conditions are optimized, the microgravity-grown crystals of certain proteins are superior to crystals obtained under comparable conditions on earth. In general, the space-grown crystals are larger and display more uniform morphologies than crystals grown under similar conditions on earth; this finding is consistent with earlier space experiments in protein crystal growth [5,6]. Analysis of three-dimensional X-ray diffraction intensity data sets for crystals of three proteins grown under microgravity conditions shows diffraction to higher resolution than the best crystals of these proteins that have been grown on earth.

The improved diffraction patterns from the space-grown crystals may not be entirely attributable to enhanced internal order of the crystals. Intensity data sets were collected in three different laboratories in order to obtain the data as rapidly

as possible after the space experiments and to collect data at locations where earth-grown crystals were routinely analyzed. Although the same type of area detector system was used in these three laboratories, there were variations in data collection procedures. However, when the results for these experiments are considered together, the data indicate that protein crystals grown under microgravity conditions diffract to higher resolution than the best crystals obtained under similar conditions on earth.

The relative-Wilson plots indicate that the space-grown crystals are more highly ordered at the molecular level than crystals grown by the same method on earth. Crystals from these proteins produce relative-Wilson plots that indicate lower overall mean-square-atomic-displacement values for the space-grown crystals. These  $B$  values would be expected to reflect thermal motion, biochemical heterogeneity, conformational heterogeneity, and deviations from ordered crystal-packing patterns. It seems unlikely that gravity could affect any of these parameters except molecular order at the lattice level. Under microgravity conditions, convective flow patterns that accompany crystal growth would be eliminated, thus generating a more controlled environment at crystal interfaces. Since protein crystals are relatively weakly bonded, with water bridges playing predominant roles, it may not be surprising that molecular-packing patterns would be more regular in the absence of convective flows.

The results that we have obtained are especially striking, since we have compared a single set of microgravity experiments with the best of extensive experiments that have been performed on the ground. A one-to-one comparison between the microgravity experiments and the corresponding control experiments performed immediately after the shuttle flight is even more dramatic. For example, we obtained only small crystals of  $\gamma$ -IFN D in the control experiments, and relatively small dendritic clusters of isocitrate lyase. The control experiments for elastase produced only crystals with dimensions less than about 0.4 mm. These results from a single set of control experiments simply emphasize the limited reproducibility that is obtained in most protein crystal growth experiments.

The advantage of the vapor diffusion system that we have selected for the shuttle experiments is that it permits us to compare limited space experiments with a vast array of data obtained by hanging-drop experiments under laboratory conditions on earth. Using this technique, we plan to extend these space experiments to include a number of other proteins, nucleic acids, and protein-nucleic acid complexes that have been studied extensively on earth by vapor diffusion methods.

#### Acknowledgements

This research was supported by NASA contract NAS8-36611 and NASA grant NAGW-813. We are grateful to D. Jex, the NASA Manager of the Protein Crystal Growth Project at the Marshall Space Flight Center, to Dr. R. Naumann of the Marshall Space Flight Center for his continuous help and support, to the engineers and program managers at Teledyne-Brown Engineering Company who designed and constructed our protein crystal growth apparatus, to the many NASA employees who helped at all stages of the shuttle activities, and to Dr. F.L. Suddath for his inval-

uable assistance in developing a space version of the hanging drop method.

#### References

- [1] L.J. DeLucas and C.E. Bugg, *Trends Biotechnol* 7 (1987) 188
- [2] C.E. Bugg, *J. Crystal Growth* 76 (1986) 535
- [3] M. Pusey, W. Witherow and R. Naumann, *J. Crystal Growth* 90 (1988) 105
- [4] R.L. Kroes and D. Reiss, *J. Crystal Growth* 69 (1984) 414
- [5] W. Littke and C. John, *Science* 225 (1984) 203
- [6] L.J. DeLucas, F.L. Suddath, R. Snyder, R. Naumann, M.B. Broom, M. Pusey, V. Yost, B. Herren, D. Carter, B. Nelson, E.J. Meehan, A. McPherson and C.E. Bugg, *J. Crystal Growth* 76 (1986) 681
- [7] A. McPherson, *Methods Enzymol* 114 (1985) 112
- [8] A.J. Howard, G.L. Gilliland, B.C. Finzel, T.L. Poulos, D.H. Ohlendorf and F.R. Salemme, *J. Appl. Cryst.* 20 (1987) 383.
- [9] T.L. Blundell and L.N. Johnson, *Protein Crystallography* (Academic Press, New York, 1976)
- [10] V.-K. Senadhi, S.E. Senadhi, S.E. Ealick, L. Tattanahalli, T.L. Nagabhushan, P.P. Trotta, R. Kosecki, P. Reichert and C.E. Bugg, *J. Biol. Chem.* 262 (1987) 4804
- [11] L. Sawyer, D.M. Shotton, J.W. Campbell, P.L. Wendell, H. Muirhead, H.C. Watson, R. Diamond and R.C. Ladner, *J. Mol. Biol.* 18 (1978) 137
- [12] Canavalin, human serum albumin, human C reactive protein, snake venom phospholipase A2, human renin, synthetic peptide, human purine nucleoside phosphorylase, HIV reverse transcriptase